# The effects of Ca<sub>14</sub>Mg<sub>2</sub>(SiO<sub>4</sub>)<sub>8</sub>:Eu<sup>2+</sup> phosphor on white light emission quality of LED-phosphor packages

## Ha Thanh Tung<sup>1</sup>, Dieu An Nguyen Thi<sup>2</sup>, Nguyen Doan Quoc Anh<sup>3</sup>

<sup>1</sup>Faculty of Basic Sciences, Vinh Long University of Technology Education, Vinh Long Province, Vietnam <sup>2</sup>Faculty of Electrical Engineering Technology, Industrial University of Ho Chi Minh City, Ho Chi Minh City, Vietnam <sup>3</sup>Faculty of Electrical and Electronics Engineering, Ton Duc Thang University, Ho Chi Minh City, Vietnam

#### **Article Info**

## Article history:

Received Nov 2, 2022 Revised Nov 16, 2022 Accepted Dec 21, 2022

# Keywords:

Ca<sub>14</sub>Mg<sub>2</sub>(SiO<sub>4</sub>)<sub>8</sub>: Eu<sup>2+</sup> Color quality Green-emitting phosphor High luminous flux White light emitting diodes

#### **ABSTRACT**

Ca<sub>14</sub>Mg<sub>2</sub>(SiO<sub>4</sub>)<sub>8</sub>: Eu<sup>2+</sup> (CMS:Eu<sup>2+</sup>) green phosphor is used for creating the white-light emitting diode (W-LED) packages with conversion phosphor materials. The phosphor shows the broadband green emission that peaks at 505 nm in the blue wavelength. The phosphor introduces the improvement in the blue and green emission spectra, which helps to heighten the luminous flux. Moreover, that the concentration of CMS:Eu<sup>2+</sup> increases, the scattering events are enhanced to benefits the color blending for lower color variations or better color uniformity. The color renditions reduce with the rising greenphosphor concentration. The green-light amount becomes surplus and redundant for balancing color elements of white light emission. Thus, it should adjust and keep the concentration of CMS:Eu<sup>2+</sup> in the range of ~2–8 wt%, to get the average number of color rendering index (CRI) (73-75), and color quality scale (CQS) (60-64). The CMS: Eu<sup>2+</sup>, hence, is suitable for white light realization, and the W-LED aiming at high-luminescence white light emission with improved color uniformity, and average rendering performances.

This is an open access article under the **CC BY-SA** license.



3388

## Corresponding Author:

Nguyen Doan Quoc Anh Faculty of Electrical and Electronics Engineering, Ton Duc Thang University Ho Chi Minh City, Vietnam.

Email: nguyendoanquocanh@tdtu.edu.vn

## 1. INTRODUCTION

The invention of light-emitting diode (LED) has introduce the potential and effective solution for the lighting industry and market since LEDs have been reported to possess many outstanding characteristics: i) the long hour of using (can be up to 50,000 hours) [1], [2], ii) the compact size that is beneficial to the large scale production as the production cost could be reduced [3], [4], iii) the lower power consumption and significantly less carbon emission that contribute to the factor of eco-friendliness [5], [6], and iv) the usefulness and effectiveness in directional lighting applications as the light can be delivered effectively to the targeted surface. Therefore, keeping and developing the advantages while overcoming the disadvantages of the LED packages are constantly the interesting topics for researchers and manufacturers [7]–[9]. The LED that emits white light is the desirable for new generation lighting solution [10], [11]. The white colored light can be perceived with the combination of blue and yellow, or blue, green, and red emission colors. The preferred packaging method to achieve a white-emission LED is using the blue-excitation chip with the high-performance conversion phosphor. This method is reported to be simpler and save the production cost than combing several different colored-emission LED chips as it does not suffer the wiring complexity, or the problems of different currents for the chips to emits sufficient spectral color the form white light. The YAG: Ce<sup>3+</sup> is the well-known yellow-emitting phosphor that was used to produce the white LED (W-LED)

from the very first day. The luminescent output of the W-LED using blue chip and YAG: Ce<sup>3+</sup> phosphor is high, yet the color rendering index (CRI) would be somehow inadequate owing to the inefficient red or lack of green color spectra [12], [13]. Thus, providing one of the two mentioned color emission spectra can help improve the CRI of the W-LED. The green phosphor with the emission band including a part of orange or red color could be good for compensating the color shortage in the white light emission, contributing to stimulating the better color rendition. The phosphor that is expected for high-performance W-LED should has broad emission band and strong absorption ability in wavelength of blue LED to effectively converted the blue light and reduce the scattering loss [14]. Thus, the broadband emission ions (Eu<sup>2+</sup> and Ce<sup>3+</sup>) could be used to satisfy this requirement. Besides, deciding the suitable host lattice for the ion dopant plays a crucial role in the optical performance of the phosphor. The alkaline earth silicate phosphor is recognized for its temperature stability, and high efficacy, and broad bandgap. When combining with Eu<sup>2+</sup> ion, this type of phosphor can give high performance [15].

In this study, the phosphor Ca<sub>14</sub>Mg<sub>2</sub>(SiO<sub>4</sub>)<sub>8</sub>: Eu<sup>2+</sup> (shortened as CMS: Eu<sup>2+</sup> or Eu<sup>2+</sup>-doped CMS) is prepared and applied to analyze its optical influences on the W-LED performances. This phosphor has green emission that peak at about 505 nm when being monitored under excitation wavelength of 400 nm. The analysis is conducted on the hue consistency, hue rendition factors, and lumen of the white illumination emission at the three different wavelengths of 6,000 K; 7,000 K; and 8,000 K. The collected data show that the CMS: Eu<sup>2+</sup> encourages the improvement of the luminous flux (LF) intensity and the color uniformity or homogeneity by increasing its concentration within the phosphor setting. In contrast, the surging concentration for CMS: Eu<sup>2+</sup> leads to the decrease in CRI as well as color quality scale (CQS). By lowering the concentration for CMS: Eu<sup>2+</sup>, the average CRI of 72–75 and CQS of 63–64 can be attained. The study shows that this green phosphor is suitable for high-luminescence white light emission with improved color uniformity, while keeping the average rendering ability.

#### 2. METHOD

## 2.1. Making green Ca<sub>14</sub>Mg<sub>2</sub>(SiO<sub>4</sub>)<sub>8</sub>: Eu<sup>2+</sup>

CMS:  $Eu^{2+}$  is synthesized using solid state method [16]. Chemical components of the required green phosphor are presented in Table 1. The raw components are blended by grinding and then burned in the reducing environment of 5%  $H_2/$  95%  $N_2$ . The burning stage is carried out at the temperature range of 1,100 °C–1,400 °C and lasts 4 h. The concentration of doped rare earth ion  $Eu^{2+}$  is determined at 0.3 mol. Characterization procedure is carried out to monitor the luminescence and crystal structure of the as-prepared  $Eu^{2+}$ -doped CMS phosphor. The Cu K(alpha) radiation (Xray diffraction pattern) of  $Eu^{2+}$ -doped CMS phosphor is measured with  $10^{\circ} \le 20 \le 100^{\circ}$  angular range and a  $0.026^{\circ}$  step size, using the diffractometer X'Pert supplied by Philips.

Table 1. Chemical components of green-emitting phosphor CMS: Eu<sup>2+</sup>

Components	Purity (%)	Purchased from
CaCO <sub>3</sub>	99.9	Sigma-Aldrich
$SiO_2$	99.9	Sigma-Aldrich
MgO	99.9	Sigma-Aldrich
$Eu_2O_3$	99.9	Sigma-Aldrich

The luminescence of the phosphor that is monitored at the room temperature is attained with the hitachi F-4,500 spectrophotometer (300–700 nm). The ultraviolet/visible/near infrared (UV/VIS/NIR) spectrophotometer model varian cary 500 would be used for measuring diffuse reflectance spectra of the phosphor with the wavelength ranging from 200 nm to 600 nm. The quantum efficacy is collected under an excitation wavelength of 400 nm using the measurement system QE-1,000 provided by Otsuka electronics. For the W-LED packaging modules, an InGaN-based LED chip, exhibiting the peak wavelength of 395 nm, is applied to excite the phosphor powders. The dimension of the chip would be 1.14×0.15 mm (square base×height). The encapsulation film placed on the chip is comprised of yellow phosphor (YAG: Ce<sup>3+</sup>), green phosphor (CMS:Eu<sup>2+</sup>), and silicone, and its thickness is about 0.08 mm. The W-LED structured model will be displayed by Figure 1.

#### 2.2. Computational analysis

With the doping amount of 0.3 mol for Eu<sup>2+</sup> ion, the prepared CMS: Eu<sup>2+</sup> phosphor emits potent green discharge focalized under 505 nm, monitored under the exciting wavelength reaching 400 nm. As the concentration of Eu<sup>2+</sup> increases, the discharge spectrum of the green phosphor tends to move to a larger wavelength band of orange color. The reabsorption factor among the doped ions is the main cause of this

3390 □ ISSN: 2302-9285

change, indicating that the change in crystal field surrounding the ions has less impact on the phosphor's emission shift. The crystal field surrounding of  $Eu^{2+}$  ions (Dq) is generally expressed in (1) [17]:

$$\Delta = Dq = (Ze^2r^4)/(6R^5) \tag{1}$$

with R shows the distance between the central Eu ion and its binding ions; Z and e indicate the charges of the anion and the electron, respectively; r means the radius and d means the wavefunction. The ionic radii of  $Ca^{2+}$  (8 coordination) and  $Eu^{2+}$  were 1.12 Å and 1.25 Å, showing that the splitting phenomenon in the crystal field does not directly and significantly cause the red-shift in the CMS: $Eu^{2+}$  emission.

The critical distance for the energy transfer between the Eu ion  $(R_c)$  in the phosphor matrix, which describes the separation between the ions that is closest to the others at a critical ion concentration  $(X_c)$ , can be expressed using (2) [18]:

$$R_c \approx 2 \left[ 3V / (4\pi X_c N) \right]^{1/3}$$
 (2)

From this equation, the essential parameters to calculate the  $R_c$  includes V is the unit cell's volume, N is the total number sites of the Eu<sup>2+</sup> ion in each unit cell, and  $X_c$ , which are 1356.5 Å<sup>3</sup>, 8, and 0.3, respectively. Consequently, the computed  $R_c$  is about 12.9 Å. The energy transfer between the ion is also influenced by the interaction mechanism. In this case, the allowed transition of Eu<sup>2+</sup> is attributed to the dipole-dipole mechanism. Thus, the critical distance can also be measured using the suggested Blasse's formulas [19]:

$$P_{SA} = \left[ (2\pi)/h \right] \left| \langle S, A * | H_{SA} | S *, A \rangle \right|^2 \int g_S(E) g_A(E) dE \tag{3}$$

$$R_c^6 = 0.63 \times 10^{28} \times [(4.8 \times 10^{-16} P)/E^4] \int f_S(E) F_A(E) dE$$
 (4)

in which, P means the Eu<sup>2+</sup> oscillator strength; E means the max spectral overlap energy which is 2.66 eV.  $\int f_S(E)F_A(E)$  indicates the spectral overlap integral, which is  $1.88 \times 10^{-2}$  eV<sup>-1</sup>. Here, the taken value for P is  $10^{-2}$  which is in relation to the wide absorption of  $4f^7 \Rightarrow 4f^65d$ . Thus, the obtained R<sub>c</sub> is equal to 14.9 Å.

According to Dexter's theory, the multipole-multipole electric interaction causes the non-radioactive power shift and electron transition among the ions  $Eu^{2+}$  in the green-emitting phosphor  $Eu^{2+}$ -doped CMS phosphor. It is because the critical distance of exchange interaction that controls the forbidden-transition energy transfer is usually approximately 5 Å, implying that this factor does not participate in controlling the energy transfer among  $Eu^{2+}$  ions. The relation of emission strength ( $I_E$ ) and doped ion concentration (C) can be demonstrated with (5) [20]:

$$I_F/C = k/(1 + \beta C^{\theta/3}) \tag{5}$$

Note that C is in connection with the self-concentration quenching of the phosphor. k and  $\beta$  mean the constants of each interaction under the same setting of excitation for a specific host lattice. If  $C \gg X_c$  the loss of nonradiative energy transfer could be owing to the multipole transfer [21]. Thus, it is possible to simplify (5) as in (6):

$$I_E/C = k_1/\beta C^{\theta/3} \tag{6}$$

here,  $k_1$  is constant;  $\theta$ =6, 8, 10 indicates electric interactivities of dipole-dipole, dipole-quadrupole, and quadrupole-quadrupole, respectively. In this case,  $\theta$  can be determined from  $-\theta/3$  which is -2.16, so the result is ~6. This indicates the dipole-dipole interaction for concentration quenching of the ion Eu<sup>2+</sup> in the prepared CMS phosphor [22].

The diffuse reflectance spectrum of the phosphor CMS:  $Eu^{2+}$  can be expressed with the relation between the absorption coefficient based on Kubelka-Munk theory (K/S) and the measured reflectance (R), as (7) [23]:

$$K/S = [(1-R)^2]/2R \tag{7}$$

The relation between the temperature quenching and the emission intensity of the phosphor CMS:  $Eu^{2+}$  can be shown via (8), which includes the computed activation energy for temperature quenching (*E*) by the Arrhenius equation [24]:

$$I(T) = I_0/[1 + A \exp\left(\frac{-E}{kT}\right)] \tag{8}$$

where I and  $I_0$  are the initial intensity and the intensity under a determined temperature (T). A indicates a constant. k symbolizes the Boltzmann constant [25].

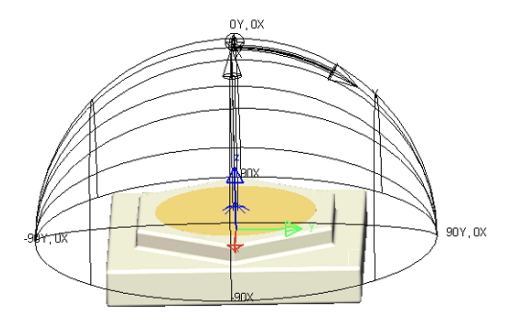
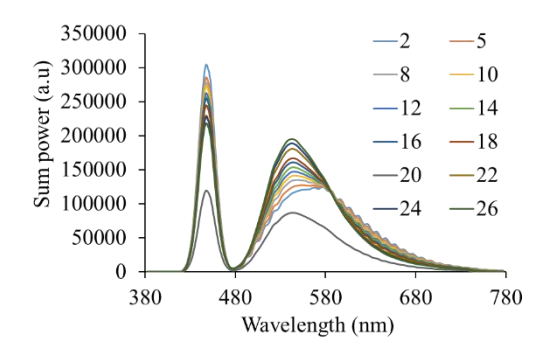


Figure 1. Illustration of the prepared WLED

# 3. RESULTS AND DISCUSSION

The emission spectra of the total W-LED package at 6,000 K, 7,000 K, and 8,000 K are demonstrated in Figures 2-4, respectively. The emission spectra clearly exhibit two emission peaks in blue and green region. It can furthermore be noticed that by modifying the concentration of CMS: Eu<sup>2+</sup> phosphor, the peak emission band in the green region could broaden to orange region. With 2 wt% CMS: Eu<sup>2+</sup>, for example, the peak emission can be observed around 570-600 nm, at all correlated color temperature (CCT) levels. When this the green-orange emission band combining with the blue emission, the human eyes could realize that combination as white light emission. Thus, the use of CMS: Eu<sup>2+</sup> phosphor is potential for white-light LED fabrication.



400000 300000 -2 -5 -8 -10 -12 -14 -16 -18 -20 -22 380 480 580 680 780 Wavelength (nm)

Figure 2. Emission spectra of 6,000 K W-LEDs regarding CMS: Eu<sup>2+</sup> weight percentages

Figure 3. Emission spectra of 7,000 K W-LED regarding CMS: Eu<sup>2+</sup> weight percentages

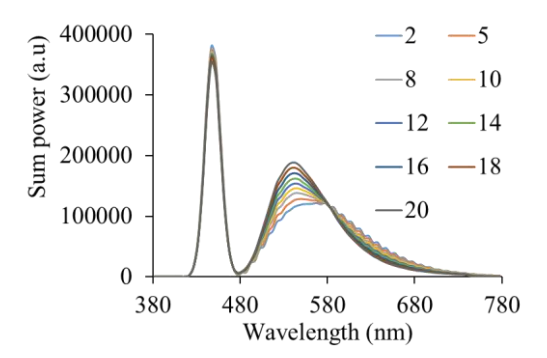


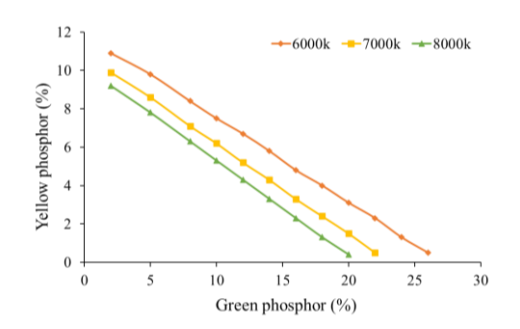
Figure 4. Emission spectra of 8,000 K W-LED regarding CMS: Eu<sup>2+</sup> weight percentages

The yellow emission of YAG: Ce<sup>3+</sup> should decrease to balance the color elements in the white light emission when the green phosphor is added to the phosphor layer. Moreover, the lesser YAG: Ce<sup>3+</sup> amount

3392 □ ISSN: 2302-9285

benefits the stability for determined CCTs of the W-LED model. That the YAG: Ce<sup>3+</sup> presence steeply decreases with the increasing concentration for green CMS:Eu<sup>2+</sup> is described in Figure 5. Besides, the stability of the CCT, the scattering property can also get advantages from this yellow-concentration reduction, leading to higher probability of the blue rays to be emitted, scattered, and transmitted through the phosphor layer to combine with the other colored lights (green and yellow). Therefore, the color uniformity can be enhanced. Accordingly, the color uniformity of the W-LED in connection with the green phosphor CMS:Eu<sup>2+</sup> concentration is examined. The evaluation is carried out based on color deviation parameter (D-CCT), in which the lower value of D-CCT indicates better color homogeneity, as demonstrated in Figure 6. In the same manner with YAG: Ce<sup>3+</sup> concentration results, the higher the concentration of green-emitting Eu<sup>2+</sup>-doped CMS phosphor, the smaller the D-CCT values, thus the more uniform the white light emission color, regardless of the W-LED's predetermined CCT. This has confirmed the benefits on color property of W-LED by adding the green phosphor Eu<sup>2+</sup>-doped CMS and getting the yellow phosphor YAG:Ce<sup>3+</sup> reduced.

The increasing phosphor concentration of CMS:Eu²+ seems to be beneficial to the hue consistency as well as LF of the W-LED. The luminous performances of the W-LED at three CCT values are illustrated in Figure 7. It is easy to observe the heightening LF in coordination with the heightening CMS:Eu²+ concentration. The highest LF values are observed to be ≥180 lm with the concentration of CMS:Eu²+ ranging from 20 to 25 wt%, which is 40-lm higher than the LF at 2 wt% CMS:Eu²+. This result can be attributed to the enhancement in the two emission bands of blue (420–480 nm) as well as green (500–580 nm) (see Figures 2–4) that may be resulted from the reduction of yellow phosphor concentration to enhance the scattering and reduce backscattering. Particularly, when the blue-light scattering is increased, the blue light has higher change to be redirected and transmitted in forward direction, allow higher proportion of light to be extracted from the W-LED phosphor package. This also reduces the energy loss caused by backscattering and reabsorption. Thus, the emission strength could be significantly enhanced.



2500 2000 2000 1500 500 0 5 10 15 20 Green phosphor (%)

Figure 5. Median CCT maintained by altering phosphor presence

Figure 6. D-CCT indices of W-LEDs regarding CMS: Eu<sup>2+</sup> weight percentages

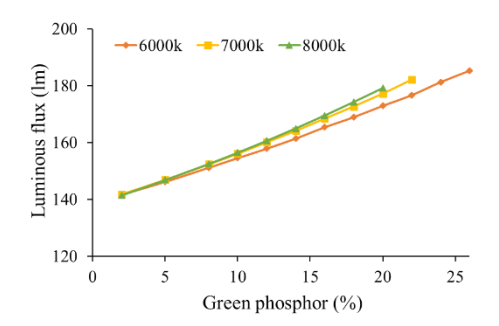
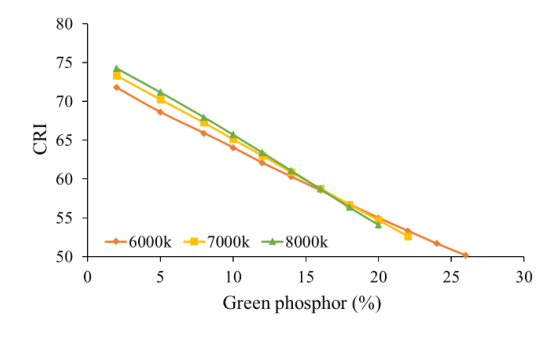


Figure 7. LF values of W-LEDs regarding CMS: Eu<sup>2+</sup> weight percentages

The color rendition features, on the other hand, does not favor the increasing CMS:Eu<sup>2+</sup> concentration. As can be seen in Figures 8 and 9, the CRI and CQS of the white light is emission is inversely proportional to the green phosphor concentration. Greater green phosphor amount leads to worse CRI and CQS, at all CCTs. This decrease of color rendering parameters mainly caused by the green-light surplus. When the amount of green phosphor rises, the yellow phosphor concentration decreases (see Figure 5), and it requires more blue lights to efficiently excite the green phosphor, consequently, the yellow and blue light proportions considerably decrease. In other word, the continuously increasing green phosphor concentration

breaks the color balance among the green, blue, and yellow colors, leading to the greenish light with lower color fidelity [26]. In the case of CQS, it initially increases when the CMS: $Eu^{2+}$  concentration rises to ~8 wt%, and then gradually decreases as the green phosphor concentration continuously increases. Meanwhile, at the same ~8 wt%, the CRI decreases to ~70 for all CCTs. The CRI of the W-LED reaches its peak with 2 wt% CMS: $Eu^{2+}$ . The CRI peaks, about 73, 74, and 75, for 6,000 K; 7,000 K; and 8,000 K, respectively, can be attained with 2 wt% CMS: $Eu^{2+}$ . With the same 2 wt% concentration of green phosphor, the attained CQS is about 63 – 64, lower than that in ~ 8wt% case. Hence, to reach the average color rendition for the white light, it is recommended to keep the  $Eu^{2+}$ -doped CMS concentration  $\leq$  8 wt%.



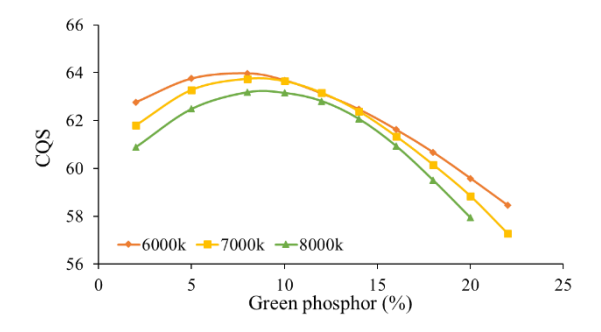


Figure 8. CRI numbers of W-LEDs regarding CMS: Eu<sup>2+</sup> weight percentages

Figure 9. CQS numbers of W-LEDs regarding CMS: Eu<sup>2+</sup> weight percentages

## 4. CONCLUSION

The green phosphor CMS:Eu<sup>2+</sup>, when added to the phosphor encapsulation layer, contributes to enhancing the emission spectra of the blue and green region, leading to significant alterations for the lumen as well as hue performances for the W-LED. High luminous efficiency and color uniformity is obtained by heightening the integrating concentration of CMS:Eu<sup>2+</sup>. The color renditions, in contrast, decrease as the green-phosphor concentration increases. The increase of the green phosphor results in the dominance of the green light, causing the insufficient proportion for blue as well as yellow illumination that would be necessary to realize the white illumination. Therefore, the attained CRI and CQS values are lowered. The recommended concentration range of CMS:Eu<sup>2+</sup> for adequate CQS and CRI is ~2–8 wt%, after considering the luminous factor.

## REFERENCES

- [1] M. Chlipala and T. Kozacki, "Color LED DMD holographic display with high resolution across large depth," *Optics Letters*, vol. 44, no. 17, pp. 4255–4258, 2019, doi: 10.1364/OL.44.004255.
- [2] K. J. Francis, Y. E. Boink, M. Dantuma, M. K. A. Singh, S. Manohar, and W. Steenbergen, "Tomographic imaging with an ultrasound and LED-based photoacoustic system," *Biomedical Optics Express*, vol. 11, no. 4, pp. 2152–2165, 2020, doi: 10.1364/BOE.384548.
- [3] S.-H. Lin et al., "Enhanced external quantum efficiencies of AlGaN-based deep-UV LEDs using reflective passivation layer," Optics Express, vol. 29, no. 23, pp. 37835–37844, 2021, doi: 10.1364/OE.441389.
- [4] R. Yoshimura, D.-H. Choi, M. Fujimoto, A. Uji, F. Hiwatashi, and K. Ohbayashi, "Dynamic optical coherence tomography imaging of the lacrimal passage with an extrinsic contrast agent," *Biomedical Optics Express*, vol. 10, no. 3, pp. 1482–1495, 2019, doi: 10.1364/BOE.10.001482.
- [5] J. Li et al., "On-chip integration of III-nitride flip-chip light-emitting diodes with photodetectors," Journal of Lightwave Technology, vol. 39, no. 8, pp. 2603–2608, 2021, doi: 10.1109/JLT.2020.3048986.
- [6] C.-M. Tsai, C.-S. Chang, Z. Xu, W.-P. Huang, W.-C. Lai, and J.-S. Bow, "Efficiency enhancement of III-nitride light-emitting diodes with strain-compensated thin-barrier InGaN/AIN/GaN multiple quantum wells," OSA Continuum, vol. 2, no. 4, pp. 1207–1214, 2019. doi: 10.1364/OSAC.2.001207.
- [7] M. Chlipala et al., "Nitride light-emitting diodes for cryogenic temperatures," Optics Express, vol. 28, no. 20, pp. 30299–30308, 2020, doi: 10.1364/OE.403906.
- [8] A. Zhang et al., "Enhanced amplified spontaneous emission from conjugated light-emitting polymer integrated with silicon nitride grating structures," OSA Continuum, vol. 2, no. 10, pp. 2875–2882, 2019, doi: 10.1364/OSAC.2.002875.
- [9] K. Tian *et al.*, "On the polarization self-screening effect in multiple quantum wells for nitride-based near ultraviolet light-emitting diodes," *Chinese Optics Letters*, vol. 17, no. 12, p. 122301, 2019, doi: 10.3788/COL201917.122301.
- [10] A. Hassan, S. Khan, K. Rasul, and A. Hussain, "Lensless on-chip LED array microscope using amplitude and phase masks," *Journal of the Optical Society of America B*, vol. 37, no. 12, pp. 3652–3659, 2020, doi: 10.1364/JOSAB.396076.
- [11] X. Gao et al., "Circularly polarized light emission from a GaN micro-LED integrated with functional metasurfaces for 3D display," Optics Letters, vol. 46, no. 11, pp. 2666–2669, 2021, doi: 10.1364/OL.415150.
- [12] S. Zhang et al., "Efficient emission of InGaN-based light-emitting diodes: toward orange and red," Photonics Research, vol. 8, no. 11, pp. 1671–1675, 2020, doi: 10.1364/PRJ.402555.
- [13] T. Zhang, X. Zhang, B. Ding, J. Shen, Y. Hu, and H. Gu, "Homo-epitaxial secondary growth of ZnO nanowire arrays for a UV-free warm white light-emitting diode application," *Applied Optics*, vol. 59, no. 8, pp. 2498–2504, 2020, doi: 10.1364/AO.385656.
- [14] H. Goo, S. Mo, H. J. Park, M. Y. Lee, and J.-C. Ahn, "Treatment with LEDs at a wavelength of 642 nm enhances skin tumor

3394 ISSN: 2302-9285

proliferation in a mouse model," Biomedical Optics Express, vol. 12, no. 9, pp. 5583-5596, 2021, doi: 10.1364/BOE.427205.

- M. V. -Treviño, J. G. -Gutiérrez, J. M. R. -Lelis, and E. L. Apreza, "Optimizing an LED array for an infrared illumination source using the near field for venous pattern detection," Applied Optics, vol. 59, no. 9, pp. 2858-2865, 2020, doi: 10.1364/AO.381815.
- V.-C. Su and C.-C. Gao, "Remote GaN metalens applied to white light-emitting diodes," Optics Express, vol. 28, no. 26, pp. 38883-38891, 2020, doi: 10.1364/OE.411525.
- [17] A. D. Griffiths et al., "Multispectral time-of-flight imaging using light-emitting diodes," Optics Express, vol. 27, no. 24, pp. 35485-35498, 2019, doi: 10.1364/OE.27.035485.
- [18] Z.-H. Xu, W. Chen, J. Penuelas, M. Padgett, and M.-J. Sun, "1000 fps computational ghost imaging using LED-based structured illumination," Optics Express, vol. 26, no. 3, pp. 2427–2434, 2018, doi: 10.1364/OE.26.002427.
- M. K. Hedili, B. Soner, E. Ulusoy, and H. Urey, "Light-efficient augmented reality display with steerable eyebox," Optics Express, vol. 27, no. 9, pp. 12572–12581, 2019, doi: 10.1364/OE.27.012572.
- [20] E. M. A. Anas, H. K. Zhang, J. Kang, and E. Boctor, "Enabling fast and high quality LED photoacoustic imaging: a recurrent neural networks based approach," Biomedical Optics Express, vol. 9, no. 8, pp. 3852-3866, 2018, doi: 10.1364/BOE.9.003852.
- [21] M. A. Khan, R. Takeda, Y. Yamada, N. Maeda, M. Jo, and H. Hirayama, "Beyond 53% internal quantum efficiency in a AlGaN quantum well at 326 nm UVA emission and single-peak operation of UVA LED," Optics Letters, vol. 45, no. 2, pp. 495-498, 2020, doi: 10.1364/OL.376894.
- H. Gu, M. Chen, Q. Wang, and Q. Tan, "Design of two-dimensional diffractive optical elements for beam shaping of multicolor light-emitting diodes," *Applied Optics*, vol. 57, no. 10, pp. 2653–2658, 2018, doi: 10.1364/AO.57.002653.

  [23] E.-L. Hsiang, Q. Yang, Z. He, J. Zou, and S.-T. Wu, "Halo effect in high-dynamic-range mini-LED backlit LCDs," *Optics*
- Express, vol. 28, no. 24, pp. 36822-36837, 2020, doi: 10.1364/OE.413133.
- [24] D. Chen et al., "Improved electro-optical and photoelectric performance of GaN-based micro-LEDs with an atomic layer deposited AlN passivation layer," Optics Express, vol. 29, no. 22, pp. 36559-36566, 2021, doi: 10.1364/OE.439596.
- W. Wang and P. Zhu, "Red photoluminescent Eu3+-doped Y2O3 nanospheres for LED-phosphor applications: synthesis and characterization," Optics Express, vol. 26, no. 26, pp. 34820-34829, 2018, doi: 10.1364/OE.26.034820.
- [26] K. Chung, J. Sui, T. Sarwar, and P.-C. Ku, "Feasibility study of nanopillar LED array for color-tunable lighting and beyond," Optics Express, vol. 27, no. 26, pp. 38229-38235, 2019, doi: 10.1364/OE.382287.

#### BIOGRAPHIES OF AUTHORS



Ha Thanh Tung ( received the Ph.D degree in physics from University of Science, Vietnam National University Ho Chi Minh City, Vietnam, he is working as a lecturer at the Faculty of Basic Sciences, Vinh Long University of Technology Education, Vietnam. His research interests focus on developing the patterned substrate with micro- and nano-scale to apply for physical and chemical devices such as solar cells, OLED, and photoanode. He can be contacted at email: tunght@vlute.edu.vn.



Dieu An Nguyen Thi 🗓 🛛 🚾 🕻 received a master of Electrical Engineering, HCMC University of Technology and Education, VietNam. Currently, she is a lecturer at the Faculty of Electrical Engineering Technology, Industrial University of Ho Chi Minh City, Vietnam. Her research interests are theoretical physics and mathematical physics. She can be contacted at email: nguyenthidieuan@iuh.edu.vn.



Nguyen Doan Quoc Anh (10 🔯 🔯 🗘 was born in Khanh Hoa province, Vietnam. He has been working at the Faculty of Electrical and Electronics Engineering, Ton Duc Thang University. Quoc Anh received his PhD degree from National Kaohsiung University of Science and Technology, Taiwan in 2014. His research interest is optoelectronics. He can be contacted at email: nguyendoanquocanh@tdtu.edu.vn.